RSC Advances

ROYAL SOCIETY OF CHEMISTRY

www.rsc.org/advances

RSC Advances

RSC Publishing

ARTICLE

Synthesis and photoswitching properties of liquid crystals derived from myo-inositol

Cite this: DOI: 10.1039/x0xx00000x

Md Lutfor Rahman,[a] Mashitah Mohd Yusoff[a] and Sandeep Kumar[b]

Received
Accepted

DOI:

www.rsc.org/advances

A new series of unconventional liquid crystals molecules derived from myo-inositol core were synthesized by linking six azobenzene units having terminal double bonds as polymerizable functional groups to myo-inositol. Differential scanning calorimetry (DSC), polarizing optical microscopy (POM) and X-ray diffraction studies were carried out to determine mesomorphism in these materials. Thus, all compounds showed stable enantiotropic SmA phase which was independent of the chain length and chain parity. The photoswitching behaviour of these molecules in solutions showed *E* to *Z* isomerization in 8-10 s, whereas the reverse process took about 270-305 min. In the solid film, the *E-Z* photoisomerization takes 5 s while the reverse transformation from *Z to E* states takes 120 min. The photoswitching behaviour of these materials represents one of the fastest switching times so far observed in such materials and, therefore, they are good candidates for molecular switches.

1. Introduction

Myo-inositol is one of the isomers of inositol which exists in nine possible stereoisomers of naturally occurring most prominent form, is *cis*-1,2,3,5-*trans*-4,6-cyclohexanehexol or *myo*-inositol, having one axial and five equatorial hydroxyl functions, is a cheap and easily available compound with stable conformational geometry of the chair conformation.[1,2] Although, the thermotropic liquid crystalline properties of inositols alkyl ethers have been studied by several researchers,[3-5] limited number of reports are seen on the liquid crystals behaviour derived from inositol molecules. Inositol-based molecules have diverse options for modification and tuning of specific properties in biological and chemical systems. The driving forces for the formation of liquid crystalline phases of amphiphilic carbohydrate derivatives are hydrogen bridges between the hydrophilic head groups and van der Waals interactions between the hydrophobic parts.[2]

Liquid crystals (LCs) are possess the ordering of crystals and also the molecular mobility of liquid.[6,7] LCs exhibit less ordering degree than solid crystals and they are classified as nematic, smectic, cholesteric and discotic type according to their special molecular arrangement.[8] By virtue of their fluidity and long-range order, LC molecules are easier to pave the way for new arrangement when they are trigger by electric field,[9] temperature,[10-12] and light.[13-18] A field of research is the photo-induced phenomenon in which the incident light brings about the molecular ordering/disordering of the liquid-crystalline system.[19] Azobenzene molecules are well known to show reversible isomerization transformations upon irradiations with UV and visible light.[20] Several oligomeric/polymeric compounds are reported with vinyl-terminated side chains mesogenic unit of cross-linked liquid crystals.[21-24]

The low and high molar mass liquid crystals containing an azo-linkage have received tremendous attention due to their unique photoswitchable properties induced by light.[25-29] Upon absorption of UV light (~ 365 nm) the energetically more stable E configuration (*trans*) converts to the Z configuration (*cis*). The reverse transformation of the Z isomer into the E isomer can be brought by irradiation with visible light (in the range of 400-500 nm). This reverse process is known as thermal back relaxation which occurs in the dark and this reverse process (*cis* to the *trans*) can occur thermally or photochemically with visible light.[30-33] This phenomenon of reversible optical switching of azobenzene functional molecules have several applications such as, in holography and data storage in various media, as the azobenzene configurational isomers are different in physical and chemical properties.[34-38] The azobenzene liquid crystals are among the most promising materials for the photochromic applications.

The present investigation focuses on the synthesis and photoisomerization behaviour of new molecules derived from *myo*-inositol core as central unit and six rod-shaped photoswitchable azobenzene units with terminal chains having double bonds as the polymerizable functional groups. For the sake of six rod-shaped photoswitchable azobenzene units with terminal chains, we anticipated that faster photoswitching property is found to be in the smectic type phase of *myo*-inositol based LCs. Therefore, we report some *E*/*Z* isomerization studied on the unconventional azobenzene compounds for possible applications in the optical data storage and molecular switches.

2. Experimental

2.1 Synthesis of intermediate compounds

All intermediate compounds **1**, **2a-e** and **3a-e** were synthesized according to our earlier paper.[30, 39]

2.2 1,2,3,4,5,6-Hexakis[4-{[4-(but-3-en-1-yloxy)phenyl]diazenyl} benzoate]cyclohexane (4a)

Compound **3a** (40 mg, 0.135 mmol), 25 mL of dry dichloromethane, DMAP (4.0 mg, 0.03 mmol), myo-inositol (4.0 mg, 0.0223 mmol) and DCC (44 mg, 0.20 mmol) were mixed and the mixture was stirred for 24 h. Work-up procedure was used according to our previous reported paper.[30] Yield of **4a**: 0.015 g (31%). IR, ν_{max}/cm^{-1} 3072 (=CH_2), 2922 (CH_2), 2852 (CH_2), 1720

(C=O, ester), 1670 (C=C, vinyl), 1647, 1456 (C=C, aromatic), 1269, 1141, 1028 (C-O), 891 (C-H). δ_H(500 MHz; $CDCl_3$; Me_4Si) 8.35 (d, 2H × 6, *J* = 8.9 Hz, Ph), 8.00 (d, 2H × 6, *J*= 8.2 Hz, Ph), 7.95 (d, 2H × 6, *J* = 8.9 Hz, Ph), 7.05 (d, 2H × 6, *J* = 8.9 Hz, Ph), 5.95 (m, 1H × 6, CH=), 5.25 (d, 1H × 6, *J* = 16.5 Hz, $=CH_2$), 5.16 (d, 1H × 6, *J* = 9.9 Hz, $=CH_2$), 4.14 (t, 2H × 6, *J* = 6.8 Hz, OCH_2-), 3.98 (s, 6H, core), 2.63 (m, 2H × 6, $-CH_2$-). δ_C(125 MHz; $CDCl_3$; Me_4Si) 34.20, 68.60, 72.60, 115.18, 118.25, 122.41, 125.24, 130.64, 131.66, 132.73, 147.23, 155.38, 162.38 and 164.44. Elemental analysis, Found: C, 70.01; H, 5.12; N, 8.99. Calc. for $C_{108}H_{96}N_{12}O_{18}$: C, 70.11; H, 5.23; N, 9.08%.

2.3 1,2,3,4,5,6-Hexakis[4-{[4-(pent-4-en-1-yloxy)phenyl] diazenyl}benzoate]cyclohexane (4b)

Compound **4b** was synthesized from **3b** according to the procedure described for the synthesis of **4a**. Yield of **4b**: 0.018 g (35%). IR, ν_{max}/cm^{-1} 3076 ($=CH_2$), 2924 (CH_2), 2852 (CH_2), 1718 (νC=O, ester), 1645 (C=C, vinyl), 1626, 1456 (C=C, aromatic), 1257, 1143, 1087 (C-O), 842 (C-H). δ_H(500 MHz; $CDCl_3$; Me_4Si) 8.36 (d, 2H × 6, *J* = 8.7 Hz, Ph), 8.01 (d, 2H × 6, *J* = 8.3 Hz, Ph) 7.99 (d, 2H × 6, *J* = 8.9 Hz, Ph), 7.05 (t, 2H × 6, *J* = 8.3 Hz, Ph), 5.88 (m, 1H × 6, CH=), 5.10 (d, 1H × 6, *J* = 9.8 Hz, $=CH_2$), 5.03 (d, 1H × 6, *J* = 9.9 Hz, $=CH_2$), 4.09 (t, 2H × 6, *J* = 6.7 Hz, OCH_2-), 3.97 (s, 6H, core), 2.30 (m, 2H × 6, $-CH_2$), 1.97 (m, 2H × 6, $-CH_2$-). δ_C(125 MHz; $CDCl_3$; Me_4Si) 29.00, 30.20, 69.00, 72.60, 115.23, 118.75, 122.65, 125.41, 130.48, 131.83, 132.66, 147.45, 155.56, 162.34 and 164.42. Elemental analysis, Found: C, 70.89; H, 6.15; N, 8.61. Calc. for $C_{114}H_{108}N_{12}O_{18}$: C, 70.97; H, 6.25; N, 8.69%.

2.4 1,2,3,4,5,6-Hexakis[4-{[4-(hex-5-en-1-yloxy)phenyl]diazenyl} benzoate]cyclohexane (4c)

Compound **4c** was synthesized from **3c** according to the procedure described for the synthesis of **4a**. Yield of **4c**: 0.020 g (37 %). IR, ν_{max}/cm^{-1} 3072 ($=CH_2$), 2922 (CH_2), 2852 (CH_2), 1718 (C=O, ester), 1643 (C=C, vinyl), 1626, 1454 (C=C, aromatic), 1246 1143, 1045 (C-O), 860 (C-H). δ_H(500 MHz; $CDCl_3$; Me_4Si) 8.36 (d, 2H × 6, *J* = 8.2 Hz, Ph), 8.01 (d, 2H × 6, *J* = 6.9Hz, Ph), 7.99 (d, 2H × 6, *J* = 6.8 Hz, Ph), 7.05 (d, 2H × 6, *J* = 8.6 Hz, Ph), 5.89 (m, 1H × 6), 5.13 (d, 1H × 6, *J* = 16.5Hz), 5.05 (d, 1H × 6, *J* = 9.9 Hz), 4.09 (t, 2H × 6, *J* = 6.7 Hz, OCH_2-), 3.97 (s, 6H, core), 2.29 (m, 2H × 6, $-CH_2$), 2.08 (m, 2H × 6, $-CH_2$-), 1.96 (m, 2H × 6, $-CH_2$-). δ_C(125 MHz; $CDCl_3$; Me_4Si) 26.11, 29.80, 33.90, 69.01, 72.60, 115.33, 118.45, 122.42, 125.31, 130.61, 131.55, 132.72, 147.13, 155.23, 162.36 and 164.40. Elemental analysis, Found: C, C, 71.19; H, 6.10; N, 8.20. Calc. for $C_{120}H_{120}N_{12}O_{18}$: C, 71.41; H, 6.01; N, 8.32%.

2.5 1,2,3,4,5,6-Hexakis[4-{[4-(hept-6-en-1-yloxy)phenyl]diazenyl} benzoate]cyclohexane (4d)

Compound **4d** was synthesized from **3d** according to the procedure described for the synthesis of **4a**. Yield of **4c**: 0.016 g (32 %). IR, ν_{max}/cm^{-1} 3061 ($=CH_2$), 2922 (CH_2), 2854 (CH_2), 1722 (C=O, ester), 1643 (C=C, vinyl), 1602, 1456 (C=C, aromatic), 1282, 1107, 1030 (C-O), 840 (C-H). δ_H(500 MHz; $CDCl_3$; Me_4Si) 8.35 (d, 2H × 6, *J* = 8.2 Hz, Ph), 8.01 (d, 2H × 6, *J* = 6.9Hz, Ph), 7.93 (d, 2H × 6, *J* = 6.8 Hz), 7.04 (d, 2H × 6, *J* = 8.6 Hz, Ph), 5.85 (m, 1H × 6), 5.07 (d, 1H × 6, *J* = 16.5Hz), 4.99 (d, 1H × 6, *J* = 9.9 Hz), 4.08 (t, 2H × 6, *J* = 6.7 Hz, OCH_2-), 3.98 (s, 6H, core), 2.12 (m, 2H × 6, $-CH_2$-), 1.97 (m, 2H × 6, $-CH_2$-), 1.86 (m, 2H × 6, $-CH_2$-), 1.70 (m, 2H × 6, $-CH_2$-). δ_C(125 MHz; $CDCl_3$; Me_4Si) 25.91, 27.78, 29.80, 34.01, 69.01, 72.60, 115.65, 118.44, 122.33, 125.35, 130.55, 131.67, 132.47, 147.26, 155.43, 162.37 and 164.43. Elemental analysis, Found: C, 71.83; H, 6.13; N, 7.85. Calc. for $C_{126}H_{132}N_{12}O_{18}$: C, 71.97; H, 6.04; N, 7.99%.

2.6 1,2,3,4,5,6-Hexakis[4-{[4-(oct-7-en-1-yloxy)phenyl]diazenyl} benzoate]cyclohexane (4e)

Compound **4e** was synthesized from **3e** according to the procedure described for the synthesis of **4a**. Yield of **4c**: 0.017 g (31.5 %). IR, ν_{max}/cm^{-1} 3074 ($=CH_2$), 2924 (CH_2), 2852 (CH_2), 1722 (C=O, ester), 1643 (C=C, vinyl), 1602, 1458 (C=C, aromatic), 1281, 1143, 1028 (C-O), 840 (C-H). δ_H(500 MHz; $CDCl_3$; Me_4Si) 8.21 (d, 2H × 6, *J* = 8.2 Hz, Ph), 7.97 (d, 2H × 6, *J* = 6.9Hz, Ph), 7.92 (d, 2H × 6, *J* = 6.8 Hz, Ph), 7.03 (d, 2H × 6, *J* = 8.6 Hz, Ph), 5.85 (m, 1H × 6), 5.05 (d, 1H × 6, *J* = 16.5Hz), 4.96 (d, 1H × 6, *J* = 9.9 Hz), 4.08 (t, 2H × 6, *J* = 6.7Hz, OCH_2-), 3.98 (s, 6H, core), 2.11 (m, 2H × 6, $-CH_2$-), 1.85 (m, 2H × 6, $-CH_2$-), 1.49 (m, 2H × 6, $-CH_2$-), 1.44 (m, 4H × 6, $-CH_2$-). δ_C(125 MHz; $CDCl_3$; Me_4Si) 25.24, 27.28, 29.12, 30.23, 34.21, 69.01, 72.60, 115.66, 118.34, 122.78, 125.33, 130.68, 131.69, 132.89, 147.27, 155.48, 162.33 and 164.44. Elemental analysis, Found: C, C, 72.39; H, 6.50; N, 7.52. Calc. for $C_{132}H_{144}N_{12}O_{18}$: C, 72.50; H, 6.63; N, 7.68%.

3. Instruments

IR spectra were recorded on a Perkin Elmer (**670) FTIR** spectrometer. ^1H NMR (500 MHz) and ^{13}C NMR (125 MHz) spectra were recorded on a Bruker (DMX500) spectrometer. The transition temperatures and their enthalpies were measured by differential scanning calorimetry (Perkin DSC 7) with heating and cooling rates of 10 °C min^{-1}. Optical textures were obtained by using Olympus BX51 polarizing optical microscope equipped with a Mettler Toledo FP82HT hot stage and a FP90 central processor unit and Olympus DP26 digital camera. X-ray diffraction measurements were carried out using Cu-Kα radiation (λ = 1.54 Å) generated from a 4 kW rotating anode generator (Rigaku Ultrax-18) equipped with a graphite crystal monochromator. Sample was filled in Hampton research capillaries (0.5 mm diameter) from isotropic phase, sealed and held on a heater. X-ray diffraction was carried out in the mesophase obtained on cooling the isotropic phase and diffraction patterns were recorded on a two-dimensional image plate (Marresearch). Though a magnetic field of about 5 k Gauss was used to align the samples, the diffraction patterns indicate that the sample was not aligned perfectly and, therefore, should be considered as unaligned sample. Absorption spectra for photochromic study were recorded using an Ocean Optics (HR4000) UV-Vis spectrometer. Myo-inositol-based photoswitchable liquid crystals were dissolved in chloroform at suitable concentrations. All solutions were prepared and measured under air in the dark at room at temperature (24 ± 1 °C) using 1 cm quartz cells. The cells were closed to avoid the evaporation of the solvent and the solutions were stirred during the irradiation time. Photoswitching behavior of the azobenzene containing myo-inositol core materials was investigated by illuminating with Exfo Acticure 4000 UV source equipped with 365 nm filter (IF 254, HgMon 365, HgMon 436 (Zeiss, Jena, Germany) generating monochromatic light as excitation source.

4. Results and discussion

4.1 Synthesis

The synthesis of compounds **4a-e** is shown in scheme 1. Compound **1** containing azobenzene containing rod-like side arms were synthesized and purified by crystallization and recrystallization from methanol with 53% yield according to our earlier paper.[39] Compound **1** was alkylated with 4-bromo-1-butene to give the ethyl 4-{[4-(but-3-en-1-yloxy)phenyl]diazenyl}benzoate **2a**, which was purified by column chromatography on silica followed by crystallization from methanol/ chloroform with 63% yield**.**

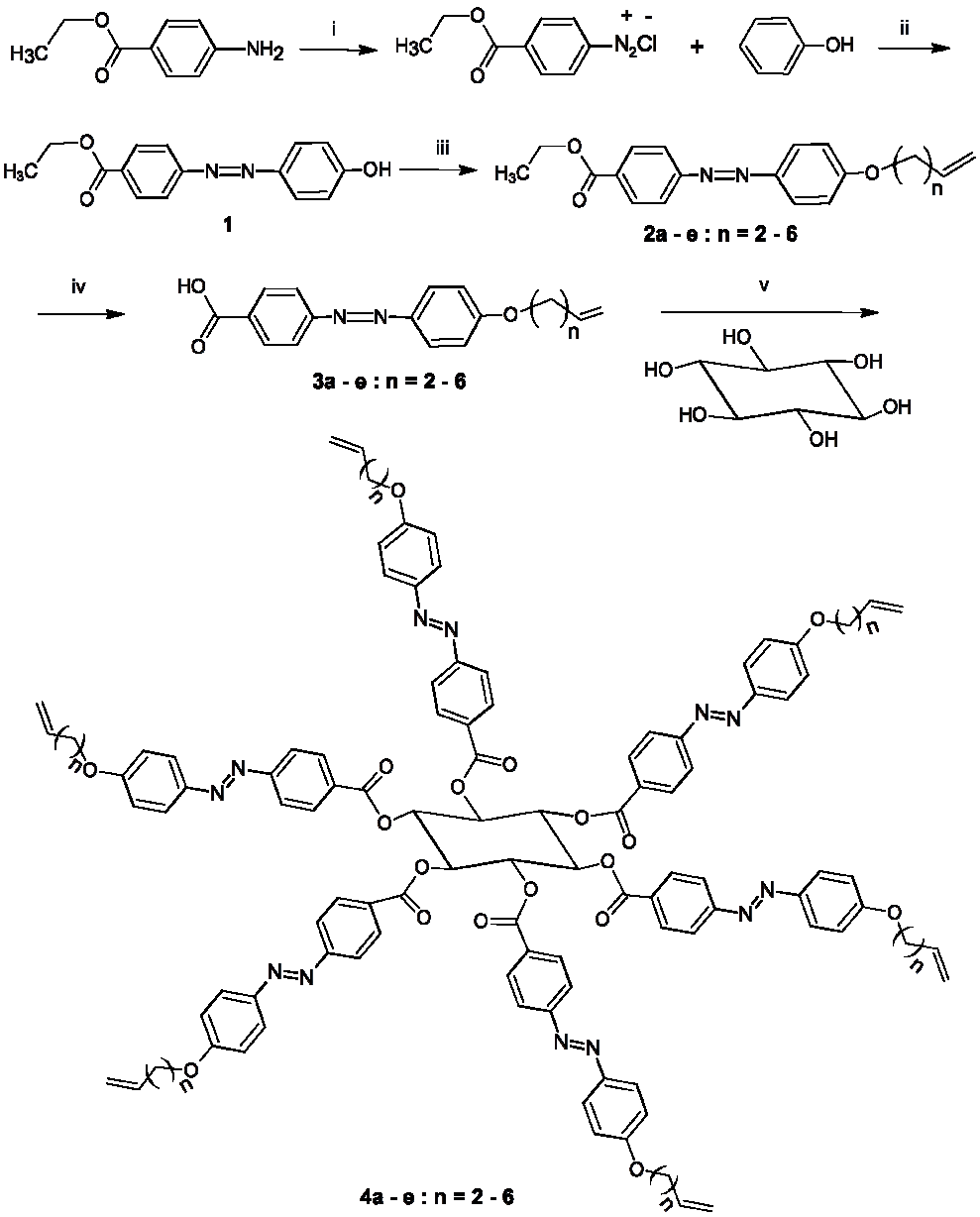

Scheme 1 Synthesis of compounds **4a-e**. Reagents and conditions: (i) $NaNO_2$, 2 °C; (ii) NaOH, pH9, 2 °C; (iii) K_2CO_3, KI, BrC_nH_{2n-1} (n = 2-6); (iv) KOH, MeOH; (v) myo-inositol, DCC, DMAP.

Table 1 Phase transition temperature (T/°C) and associated transition enthalpy values (ΔH/J g^{-1}) in parentheses given for the second heat and cooling of DSC scans for **4a-e.**

Compound	n	Heating	Cooling
4a	2	Cr 81.5 (42.3) SmA 104.7 (12.5) I	I 102.6 (12.4) SmA 77.2 (34.2) Cr
4b	3	Cr 72.7 (52.9) SmA 101.7 (14.7) I	I 99.6 (14.3) SmA 67.8 (24.2) Cr
4c	4	Cr 74.6 (56.9) SmA 95.8 (11.5) I	I 94.4 (11.9) SmA 57.0 (47.8) Cr
4d	5	Cr 71.7 (44.5) SmA 92.3 (10.8) I	I 91.2 (10.4) SmA 60.5 (40.2) Cr
4e	6	Cr 70.2 (62.9) SmA 93.5 (12.5) I	I 92.1 (13.4) SmA 62.8 (55.2) Cr

Abbreviations, Cr = crystal, SmA = smectic A phase, I = isotropic phase

Other compounds **(2b-e)** were also synthesized from the corresponding bromoalkene with the same method of compound **2**a in good overall yield up to 66%.[30] Hydrolysis of compounds **2a-e** under basic conditions yields 4-{[4-(alkyl-en-1-yloxy)phenyl]diazenyl}benzoic acid **3a-e**. Consequently, 4-{(E)-2-[4-(but-3-en-1-yloxy)phenyl]diazen-1-yl}benzoic acid **3a** was obtained as good crystals from column chromatography using methanol/dichloromethane mixture (1:10) on silica gel followed by recrystallization from methanol. The single crystal analytical data of **3a** is reported in Acta Crystallographica.[40] The acid compounds **3a-e** were coupled with hexahydroxy myo-inositol using DCC and DMAP to yield desired molecules **4a-e** as shown in Scheme 1.[41] All compounds were purified on silica gel by column chromatography followed by recrystallization. The synthesized compounds were characterized by ^{1}H, ^{13}C NMR and elemental analyses. Spectroscopic and analytical data were found to be in good agreement with the structures (see detailed synthetic procedures and analytical data in experimental section).

4.2 Mesomorphic properties

4.2.1 Differential Scanning Calorimetry (DSC)

DSC studies confirmed the phase transition temperatures (T/°C) observed by polarizing microscopy and gave the enthalpy changes (ΔH/ J g^{-1}) associated with these phase transitions. On heating, compound **4a** showed two peaks which correspond to the Cr–SmA and SmA-I transitions. On cooling, again two transition peaks appeared, indicating the existence of an enantiotropic mesophase (Table 1). On heating, compound **4b** displayed the Cr–SmA and SmA-I transitions with 3 °C lower isotropic transition temperatures than **4a**. On cooling of **4b**, again two peaks were observed corresponding to I– SmA and SmA-Cr transitions having about 3 °C lower transition temperatures from isotropic phase than **4a**. Compound **4c-e** showed similar trend showing Cr-SmA and SmA-I transitions on heating and I-SmA and SmA-Cr transitions on coolong (Table 1). DSC results observed for compound having higher alkyl groups C8 gave around 11 °C lower SmA-I transition temperatures than lower homologues C4. Similar trend on cooling cycles was observed. All the compounds are shown quite similar enthalpy values for smectic-isotropic transition. A representative DSC graph is presented in the ESI (see Fig. S1).

4.2.2 Polarizing Optical Microscopy (POM) studies

Upon heating, compound **4a** showed fan-shaped texture which is a typically smectic A phase texture. On cooling from isotropic phase, the fan-shaped texture was reformed and on further cooling only crystallization occurs at 77 °C (Fig. 1). Compound **4b** showed focal conic texture at about 5 degrees lower transition temperature than **4a**. On the other hand, compound **4c** showed the pseudo fan-shaped texture which was anticipated for a smectic type phase. It was further characterized as SmA phase by X-ray diffraction analysis. Compound **4d** and **4e** also exhibited typical fan-shaped texture of smectic A phase. Therefore, the mesophase formation is independent of chain parity. The extinction crosses are parallel to polarizer and analyzer which indicate non-tilted smectic phases for all compounds **4a-e**. Upon shearing, homeotropic alignment was achieved and these homeotropically aligned regions showed complete darkness which is confirming the presence of a uniaxial SmA phases for these compounds **4a-e**. Typical textures of **4a-c** are shown in Fig. 1 (Textures of other compound **4d** and **4e** are shown in Fig. S2 in the ESI). The transition temperatures observed under POM were matching with DSC data. The phase structures were further characterized by X-ray diffraction analysis for a representative compound.

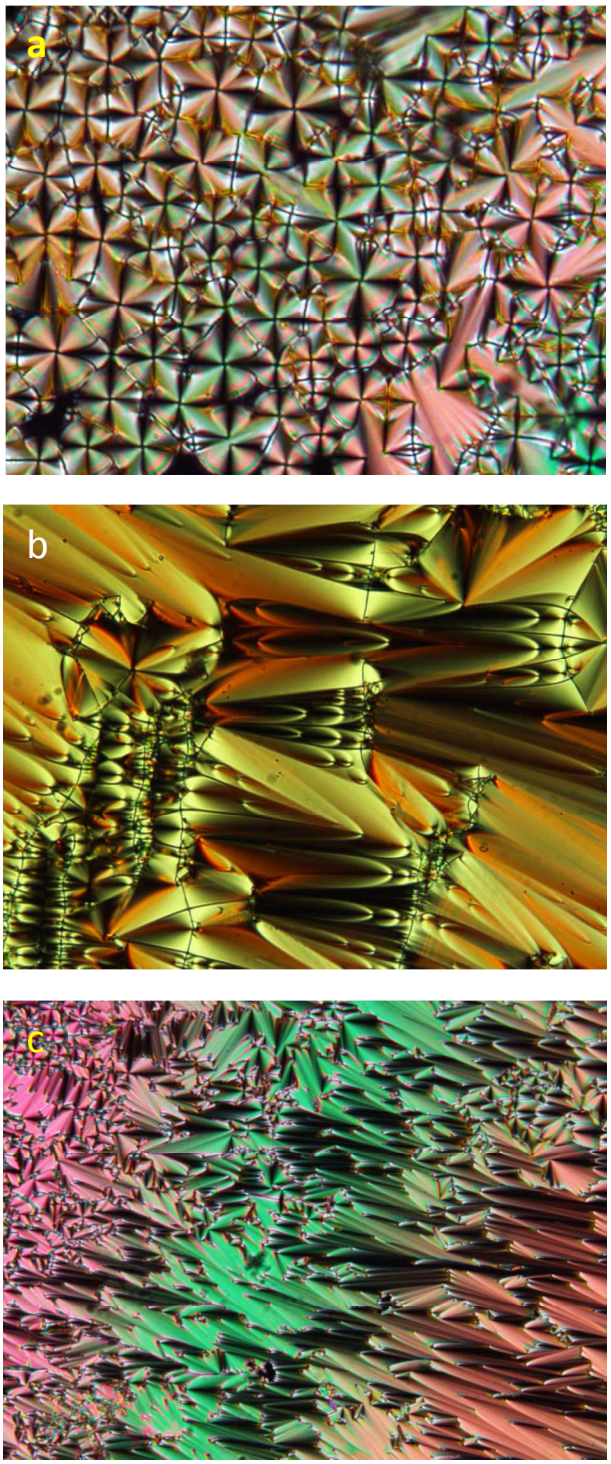

Fig. 1 Polarizing optical micrographs of (a) compound **4a** at 90 °C; (b) compound **4b** at 85 °C; (c) compound **4c** at 82 °C. All textures were captured with 10 × objective in Olympus BX51 at horizontal picture width 200 μm by Olympus DP26 camera.

4.2.3 X-ray studies

X-ray diffraction studies confirm the phase assignment. Though a magnetic field of about 5 k Gauss was used to align the samples, the diffraction patterns indicate that the sample was not aligned perfectly and, therefore, should be considered as unaligned sample. Fig. 2(a) shows the X-ray diffraction pattern of **4c** as representative 2D X-ray of this series. The X-ray pattern in the smectic A phase of **4c** at 85 °C, the arc spots in the small angle region are smeared to form a closed ring (Fig. 2a).

The intensity versus 2θ plot derived from the diffraction patterns of the compounds **4a-e** is shown in Fig. 2b. The X-ray diffractions were carried out in the mesophase obtained on cooling the isotropic phase. The diffraction patterns of all compound **4a-e** showed a sharp reflection for all compounds in the small angle region, corresponding to d = 21.24–26.66 Å, which is bit more than one half of the molecular length of **4a-e**, respectively. In other word, the layer distance is a bit less than one half of the molecular length in a conformation as shown in Fig. 3(a.b). The average molecular length (L) is estimated about 39.9–50.01 Å for compounds **4a-e** (Table 2). A small peak is observed for all compounds (**4a-e**) at d = 10.76 - 13.37 Å and in the wide-angle range a diffuse peak (d≈ 4.51 - 4.11Å) was observed. Therefore, we assume that compounds **4a-e** exhibits a smectic A intercalated phase which is denoted as $SmA_{intercal}$ phase.

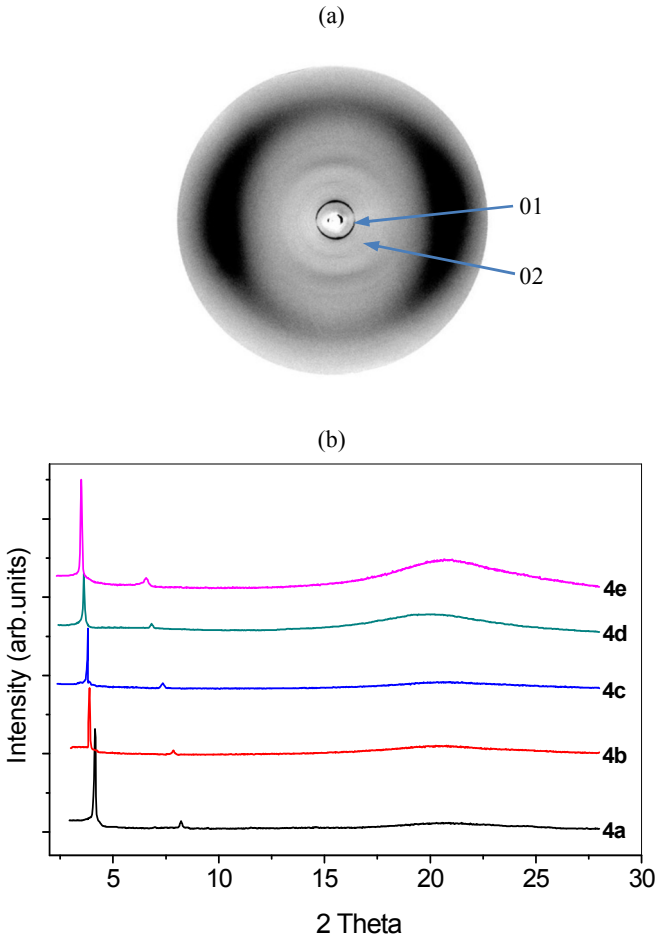

Fig. 2 (a) X-ray diffraction pattern of the compound **4c** at 82 and 85 °C (in the smectic A phase) and (b) intensity *versus* 2θ graph derived from the X-ray diffraction for the $SmA_{intercal}$ phase of compound **4a, 4b, 4c, 4d** and **4e** at 91, 88, 85, 82 and 80 °C, respectively.

Table 2. X-ray Diffraction data for compound **4a-e**

Compound	L, Å	theta, θ°	d-spacing, Å (hk)
4a	39.90	2.07	21.24 (01)
		4.10	10.76 (02)
		9.82	4.51 (halo)
4b	42.46	1.94	22.72 (01)
		3.90	11.31 (02)
		10.01	4.42 (halo)
4c	45.04	1.82	24.20 (01)
		3.66	12.04 (02)
		10.27	4.31 (halo)
4d	47.52	1.72	25.65 (01)
		3.41	12.91 (02)
		10.41	4.26 (halo)
4e	50.01	1.65	26.66 (01)
		3.30	13.37 (02)
		10.79	4.11 (halo)

The smectic phase of **4a-e** displayed the typical X-ray patterns for a SmA phase, strong layer reflections with their second order on the meridian and a diffuse outer scattering with maxima on the terminal of the pattern. The outer diffuse scattering with its maximum at d = 4.51 - 4.11 Å which indicates a liquid-like disorder of the molecules within the layers with their long axes on average parallel to the layer normal. The layer spacing of d = 21.24 - 26.66 Å estimated as one half of the molecular length for **4a-e**, these length are too shorter than the average molecular length of 39.9 - 50.01 Å, but little longer than one half of the molecular length estimated by molecular modelling of the compounds **4a-e.** Such a short layer distance could be possibly explained by partial intercalation of essentially linear molecules (Fig. 3b). At a glance the molecules resembles a cyclic type but the cyclohexane core exhibit chair-form and ultimately molecules are stretched to rod-shaped, which gave smectic A type phase for all molecules irrespective of chain length and parity.

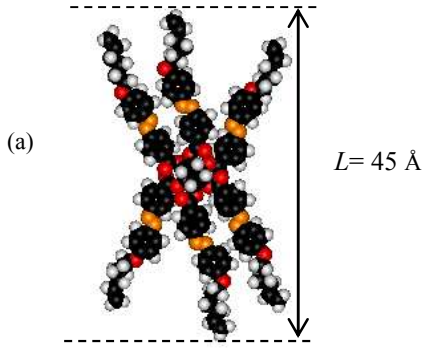

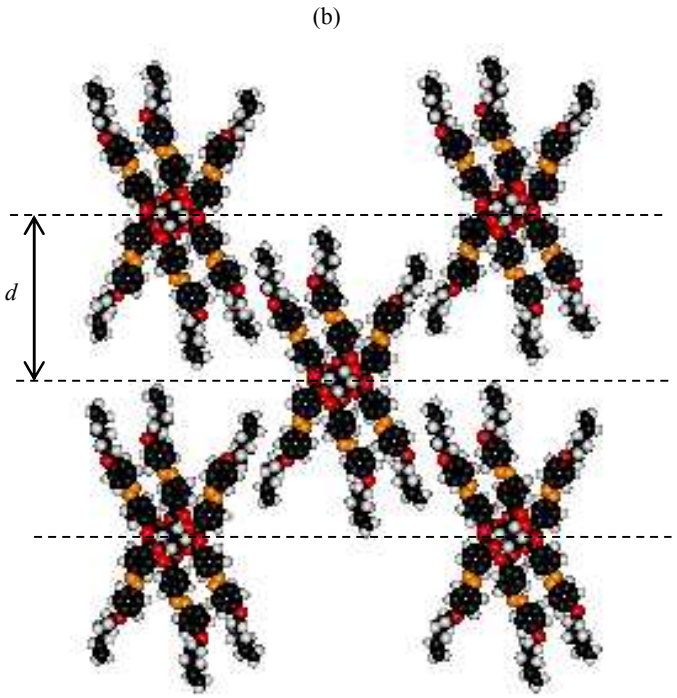

Fig. 3 (a) CPK-models of molecular conformations of compound **4c** and (b) schematic drawings of the molecular organization in the SmA phase of compounds **4a-e**. Model has been constructed from the molecular structure of compounds **4a-e** and possible schematic packing in the SmA phase for molecules with preferably rod-shaped.

4.3 Photoswitching studies

The photoswitching studies were initially carried out on solution and then on liquid crystal cells. Thus, the materials behaviour with respect to UV light is obtained and results are extremely important and necessary to create optical storage devices. All *myo*-inositol-based azobenzene molecules (**4a-e**) showed similar absorption spectra due to their similar molecular structure with variable alkyl side chains (n = 2–6), which induced little variation of the electronic transitions. However, we performed some comparison study of photoswitching property among five compounds (**4a-e**). Thus **4a-e** were dissolved in chloroform using concentration at c = 1.1×10^{-5} mol L^{-1} and the absorption spectra of all compounds before and after UV illumination is shown in Fig. 4 for **4a** and in Fig. S3 in the ESI for **4b-e**. The absorption maxima at 364 nm (π-π* transition) is the characteristic peak of *E* isomer and also a weak absorption maxima at 450 nm (n-π* transition) in the visible region is the characteristic peak of *Z* isomer.

The photoswitching properties of the compounds were studied in chloroform followed by measuring absorbance with and without light. UV light of wavelength 365 nm together with heat filter (to avoid heat radiation) was illuminated onto the sample with different time intervals until they reach pohotosaturation state. The photosaturation was observed around 9, 8, 10, 9 and 10 seconds for compounds **4a, 4b, 4c, 4d** and **4e**, respectively, absorption spectra for **4a** is shown in Fig. 4 and **4b-e** are shown in Fig S3. Due to *E/Z* photoisomerization, level of absorbance decreases which leads to the transformation of *trans*isomer to *cis* isomer (*E* to *Z*).

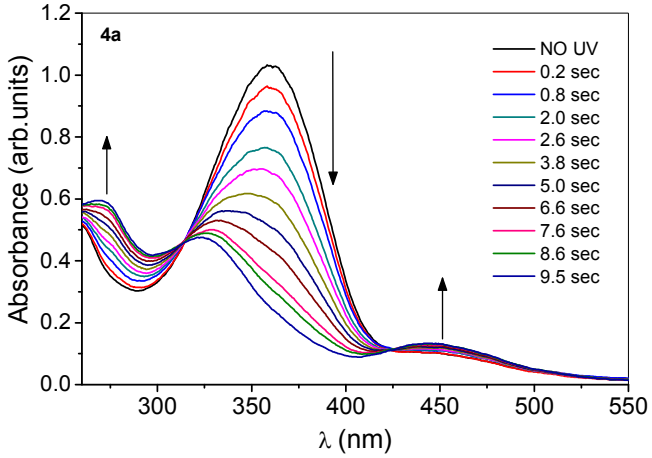

Fig. 4 Absorbance spectra of **4a** in solutions when UV light (365 nm) is shined on materials, it is evident that photosaturation occurs about ~9 seconds. Data were taken before shining UV light (NO UV) and with subsequent time intervals (UV ON). Conditions: c = 1.1×10^{-5} mol L^{-1} in in chloroform at room temperature (24 °C).

The *E-Z* absorption of compounds **4a-e** as a function of exposure time is depicted in Fig. 5. Data is derived from Fig. 4 and Fig. S3 (ESI). The absorption values were recorded at fixed wavelength 364 nm as function of exposure time with UV intensity being fixed at 5mW/cm^2. The curves in Fig. 5 showed that about 75% *E-Z* transformation occurs in 6 seconds and photosaturation occurs within 9 seconds for **4a**. In case of **4b**, the photosaturation occurred within 10 seconds. This *E-Z* transformation is fast as compared with nematic to isotropic phase involved photoisomerization.[42] The reverse transformation from *Z* to *E* can be carried out by keeping the solution in dark (thermal back relaxation).

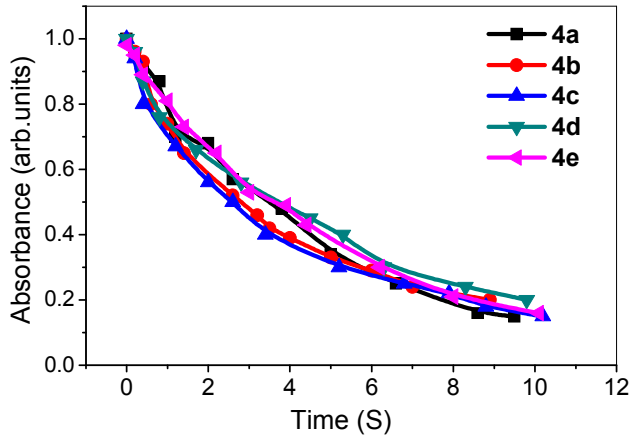

Fig. 5 Photoisomerization curve (**4a-e**) as a function of UV illumination time showing *E* to *Z* behaviour and other conditions as in Fig. 4.

The thermal back relaxation process of compounds **4a-e** were studied by shining the solution for 20 seconds to achieve photostationery state (see Fig. 5 for photostationery values) followed by leaving the solution in dark and collecting spectral data at various time intervals. Thermal back relaxation for the compound **4a** is shown in Fig. 6 and 4b-e is shown in Fig S4 in the ESI. The process took ranging from 270 to 305 min which is reasonably slow for devise fabrication.

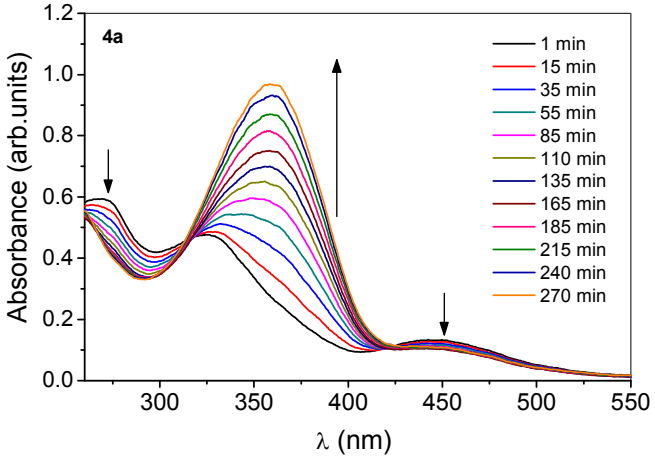

Fig. 6 The thermal back relaxation process for the compound **4a.** The UV wavelength 365 nm is shined until they reach photosaturation and subsequently data were recorded in dark state. It takes around 270 minutes to relax back to their original state. Conditions: c = 1.1 × 10^{-5} mol L^{-1} in in chloroform at room temperature (24 °C).

The time dependence photoisomerization (*Z-E* absorption) of compounds **4a-e** is shown in Fig. 7. The data for Fig. 7 is obtained from Fig. 6 and Fig. S4 (ESI) in which the absorption value is plotted as a function of recovery time at 364 nm peak wavelength. As can be seen in the Fig.7, 270, 290, 300, 302 and 305 minutes were time taken to relax back to their original state for the compounds **4a, 4b, 4c, 4d** and **4e**, respectively, which is relatively slow as compared with nematic to isotropic phase involved thermal back relaxation.[43] Prasad et al.[43] reported that the faster thermal back relaxation is due to their layered structure since changes are confined to in-plane rotation of the molecules as compared with nematic to isotropic phase involved transition. This hypothesis is well-established by the fact that a similar feature was observed in another case wherein the two phases involved have a layer structure.[43]

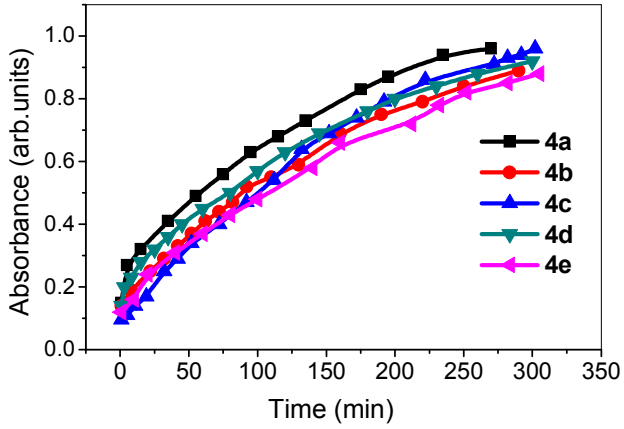

Fig. 7 Photoisomerization curve of *Z* isomer (**4a-e**) as a function of recovery time when UV light is illuminated until it reaches photosaturation and followed by measuring back relaxation time. Conditions: c = 1.1 × 10^{-5} mol L^{-1} in in chloroform at room temperature (24 °C).

We also calculated the rate constant (kt) for the *cis-trans* isomerization behaviour at room temperature for all five compounds according to the equation (1) proposed by Tsutsumi et al.[44]

$$\ln \frac{A_\infty - A_t}{A_\infty - A_0} = -kt \qquad (1)$$

Where A_t, A_0 and A_∞, are the absorbance at 365 nm of time t, time zero and infinite time, respectively. Fig. 8 shows typical first order plot using equation (1) at room temperature (24°C) for all five compounds. It is evident that throughout the relaxation time curve showed typical first order behaviour. All five compounds irrespective of their terminal alkyl chains length behaved in the similar fashion at room temperature. It is evident that all compounds showed first order exponential decay in solutions. The rate constant for the *Z-E* isomerization of 2.29 × 10^{-4}, 1.75 × 10^{-4}, 2.02 × 10^{-4}, 1.91 × 10^{-4} and 1.71 × 10^{-4} s^{-1} for **4a-e**, respectively were observed and rate constants are not substantial varied with respect to the alkyl chain length (n = 2–6).

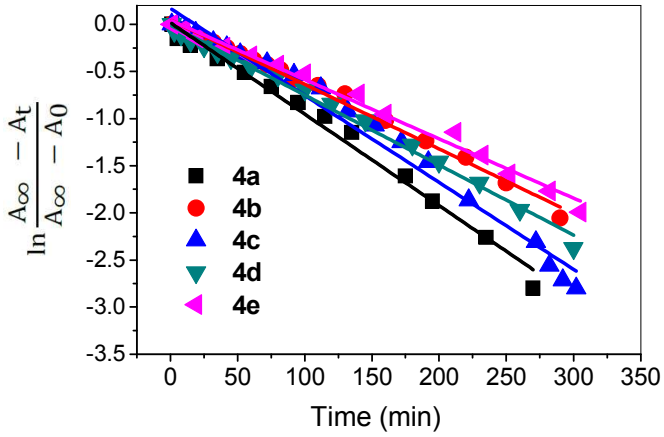

Fig. 8 First order plots for the compounds **4a-e** for *cis-trans* isomerization. Conditions: c = 1.1 × 10^{-5} mol L^{-1} in in chloroform at room temperature (24 °C).

UV-visible absorption investigations on solid films were also performed as a function of UV illumination exposure time. To elucidate the effect of azo-dyes on liquid crystals, we made solid cell filled up with **E7**, a room temperature nematic liquid crystal, as a host molecules and our *myo*-inositol liquid crystals as guest molecules. The polyimide coated, unidirectionally rubbed sandwiched cell was filled with the guest-host mixture at isotropic temperature of the mixture (~60 °C). UV/Vis spectral data were recorded using spectrophotometer as shown in Fig 9(a) and (b).

The absorption spectra of solid film on UV ON and UV OFF process for the compound **4b** are shown in Fig. 9(a) and (b), respectively**.** Peak wavelength is ~364 nm and data is generated from peak absorbance at 364 nm as a function of exposure time. It can be clearly observed that E-Z conversion took place around 5 seconds whereas recovery to the original state (thermal back relaxation) took place around 120 minutes.

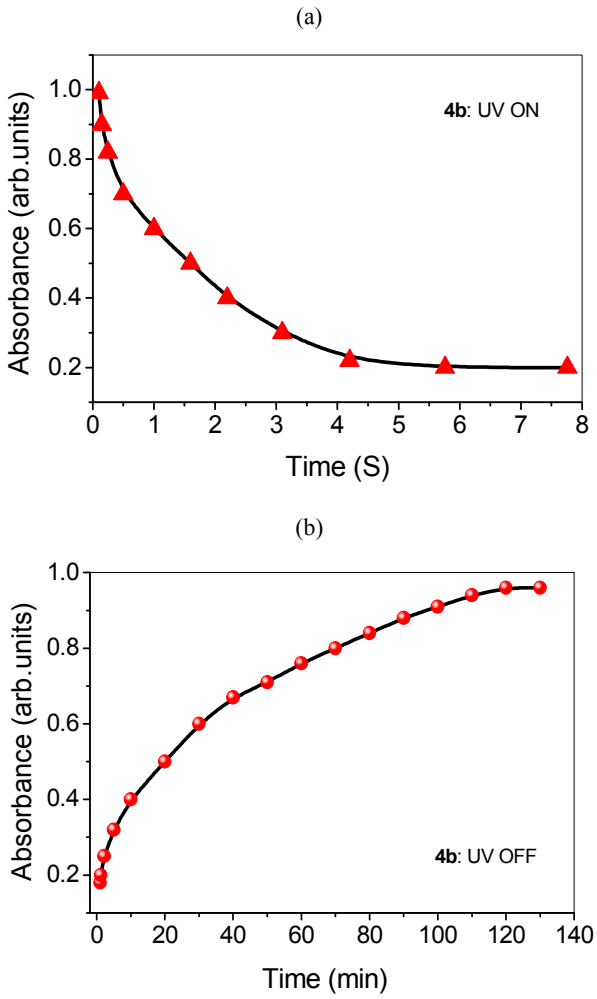

Fig. 9 (a) Time dependence photoisomerization curve of *E* isomer of **4b** shows UV ON process and (b) time dependence photoisomerization curve of **4b** for the thermal back relaxation. Conditions: E7 = 95%, compound **4b** = 5% at room temperature (24 °C).

4.4 Comparison of mesophase and photoisomerization behaviour

Myo-inositol derivatives were primarily studied for their biological properties, however, a few reports on the liquid crystalline properties were also known.[1-5] Dirk et al.[2] reported the syntheses of new regiochemically defined inositol monoethers and monoesters as well as regioisomeric inositol ester mixtures and investigated their amphitropic liquid crystallinity. All compounds showed SmA phase in this series and another series of *myo*-inositol-based compounds having liquid crystalline properties were also reported.[45] Dirk et al.[2] also remarked that myo-inositol molecules have advantage rather than a drawback, because of designing and tuning of properties via the molecular structures such as the cyclic and acyclicmono-, di-, or oligosaccharides which caused form thermotropic liquid crystal phases if they carry at least one suitably long side chain and if the head group has enough free hydroxyl groups. A various mesophases such as smectic, columnar, or cubic mesophases are commonly observed in the specific molecular constitution and shape of carbohydrate amphiphiles.[46] Compared to our synthesized *myo*-inositol-based LCs, these azobenzene-linked molecules exhibited only enantiotropic SmA phase which was independent of the chain length and chain parity. However, our main goal on the study of photoswitching properties and ultimate expectation was to be suitable switching properties, which could help in molecular switch device fabrication.

To the best of our knowledge, any photoswitching property on *myo*-inositol-based azobenzene molecules has so far not been reported. Therefore, azobenzene-linked *myo*-inositol-based liquid crystals could be considered to be new molecules for photoswitching behaviour. The photoisomerization studies reveal that the compounds **4a** intensify isomerization properties with *E* to *Z* and *Z* to *E* isomerization taking place at ranging 8-10 seconds and 270-305 min, respectively. We have anticipated that the time taken for the photoisomerization depends on the core molecules, though previous report based on the nature of the linking group (electron withdrawing group/donating group) and size of the substituent in the azobenzene moiety.[17, 27]

5. Conclusion

Five new unconventional liquid crystalline compounds having azobenzene units with terminal double bond which can be used for preparation of polymers or silyl-functionalized mesogens are prepared and characterized. These, *myo*-inositol-based monomeric compounds exhibited intercalated smectic A phase. The presence of the azo linkage in these liquid crystal monomers is suitable for photochromism studies. The photoswitching properties of compounds **4a-e** of this series show *trans* to *cis* isomerization in the ranging 9-10 seconds; the reverse process takes place at ranging 270-305 min in solution. Whereas in solids state, *E-Z* photoisomerization of **4b** takes about 5 seconds and back to original state in about 120 min. The photoswitching behaviour of these materials may be suitably exploited in the field of optical data storage device and in molecular switches which needs fast switching. So far, hardly any azo compound is reported which exhibits such a fast switching property in solid state.

Acknowledgment

This research was supported by PRGS Research Grant (No: RDU 130803). Thank Mrs. K. N. Vasudha for supporting this work.

Notes and references

[a]*Faculty of Industrial Sciences & Technology, Universiti Malaysia Pahang, 26300 Gambang, Kuantan, Pahang, Malaysia. Fax: +609 5492766; Tel: +609 5492785; E-mail: lutfor73@gmail.com*
[b]*Raman Research Institute, C.V. Raman Avenue, Sadashivanagar, Bangalore 560080, India*

† Electronic Supplementary Information (ESI) available: [materials, representative DSC graphs, POM and UV/vis absorption spectra]. See DOI: 10.1039/b000000x/

1 (a) B. V. Potter,*Nat. Prod. Rep.,* 1990, **7**, 1-24; (b) D. C. Billington, *Chem. Soc. Rev.* 1989, **18**, 83-122.
2 B. Dirk, B. Nils, S. Cosima and G. Valeria, *Langmuir*, 2009, **25**, 7872-7878.
3 D. Blunk, P. Bierganns, N. Bongartz R. Tessendorf and C. Stubenrauch, *New J. Chem.,* 2006, **30**, 1705-1717.
4 G. Catanoiu, V. Gärtner, C. Stubenrauch and D. Blunk, *Langmuir*, 2007, **23**, 12802-12805.
5 (a) H. Prade, R. Miethchen and V. Vill, *J. Prakt. Chem.,* 1995, **337**, 427-440; (b) K. Praefcke, D. Blunk and J. Hempel, *Mol. Cryst. Liq. Cryst. Sci. Technol. Sect. A.,* 1994, **243**, 323-352.

6 D. Demus, J. Goodby, G. W. Gray, H. W. Spiess and W. Vill, *Handbook of Liquid Crystals*: Wiley-VCH: Weinheim, 1998.
7 G. Wang, M. Zhang, T. Zhang, J. Guan and H. Yang, *RSC Advances*, 2012, **2**, 487-493
8 G. W. Gray, *Thermotropic Liquid Crystals*: Wiley: Chichester, 1987.
9 E. Smela, *Adv. Mater*., 2003, **15**, 481-496.
10 C. J. Legge and G. R. Mitchell, *J. Phys. D: Appl. Phys.,* 1992, **25**, 492-499.
11 K. Maeda, H. Mochizuki, M. Watanabe and E. Yashima*, J. Am. Chem. Soc.*, 2006, **128**, 7639-7650.
12 S. Kurihara, T. Ikeda and S. Tazuke, *Mol. Cryst. Liq. Cryst.,* 1990, **178**, 117-132.
13 D. Pijper, M. G. M. Jongejan, A. Meetsma and B. L. Feringa, *J. Am. Chem. Soc.*, 2008, **130**, 4541-4552.
14 D. Pijper and B. L. Feringa, *Soft Matter.,* 2008, **4**, 1349-1372.
15 Y. Yu, T. Ikeda and J. Photochem, *J. Photochem. Photobiol. C*, 2004, **5**, 247-265.
16 T. Ikeda, T. Miyamoto, S. Kurihara, M. Tsukada and S. Tazuke, *Mol. Cryst. Liq. Cryst..,* 1990, **182**, 357-371.
17 T. Ikeda, T. Miyamoto, S. Kurihara, M. Tsukada and S. Tazuke, *Mol. Cryst. Liq. Cryst*., 1990, **188**, 207-222.
18 M. M. Green, S. Zanella, H. Gu, T. Sato, G. Gottarelli, S. K. Jha, G. P. Spada, A. M. Schoevaars, B. L. Feringa and A. Teramoto, *J. Am. Chem. Soc.,* 1998, **120**, 9810-9817.
19 (a) S. K. Prasad, G. Nair and H. Gurumurthy, *Adv. Mater.*, 2005, **17**, 2086-2091; (b) D. Tanaka, H. Ishiguro, Y. Shimizu and K. Uchida, *J. Mater. Chem.*, 2012, **22**, 25065-25071; (c) E. Westphal, I.H. Bechtold and H. Gallardo, *Macromol.*, 2010, **43**, 1319-1328; (d) Y. Norikane, Y. Hirai and M. Yoshida, *Chem. Commun.*, 2011, **47**, 1770-1772.
20 T. Ikeda and O. Tsutsumi, *Science,* 1995*,* **268**, 1873-1875.
21 D. M. Walba, E. Korblova, R. Shao, J. E. Maclennan, D. R. Link, M. A. Glaser and N. A. Clark, *Science*, 2000, **288**, 2181-2184.
22 L. H. Wu, C. S. Chu, N. Janarthanan and C. S. Hsu, *J. Polym. Res.,* 2000, **7**, 125-134.
23 M. G. Tamba, A. Bobrovsky, V. Shibaev, G. Pelzl, U. Baumeister and W. Weissflog*, Liq. Cryst.,* 2011, **38**, 1531-1550.
24 D. Shen, S. Diele, I. Wirt and C. Tschierske, *Chem. Commun*., 1998, 2573-2574.
25 C. Ruslim and K. Ichimura, *J. Mater. Chem*., 1999, **9**, 673-681.
26 A. Urbas, V. Tondiglia, L. Natarajan, R. Sutherland, H, Yu, J.-H. Li and T. Bunning, *J. Am. Chem. Soc*., 2004, **126**, 13580-13581.
27 K. Ichimura, S.-K. Oh and M. Nakagawa, *Science*, 2000, **288**, 1624–1626.
28 L. Komitov, K. Ichimura and A. Strigazzi, *Liq. Cryst*., 2000, **27**, 51-55.
29 L. Komitov, C. Ruslim, Y. Matsuzawa and K. Ichimura, *Liq. Cryst*., 2000, **27**, 1011-1016.
30 M. R. Lutfor, G. Hegde, M. Y. Mashitah, M. A.M. Nor Fazli, H. T. Srinivasa and S. Kumar, *New J. Chem*., 2013, **37**, 2460-2467.
31 T. Ikeda, S. Horiuchi, D.B. Karanjit, S.Kurihara and S. Tazuke, *Macromol.*, 1990, **23**, 36-42.
32 I. Janossy and L. Szabados, *J. Non. Opt. Phys. Mater*., 1998, **7**, 539-551.
33 Y. Yu, M. Nakan and T. Ikeda, *Nature*, 2003, **425**, 145-145.
34 T. Ikeda, *J. Mater. Chem*., 2003 ,**13**, 2037-2057.
35 L. Quan, L. Lanfang, K. Julie, H.-S. Park, W. Jarrod*, Chem. Mater.*, 2005, **17**, 6018-6021.
36 S. Muhammed, O. Jesper , T. Helena, S. Kent and K. Mikhail, *Liq. Cryst.,* 2005, **32**, 901-908.
37 L. Jui-hsiang, Y. Po-chih, W. Yu-kan and W. Chien-chih , *Liq Cryst.*, 2006,**33**, 237-248.
38 L. Jui-hsiang and Y. Po-chih, *Liq. Cryst.,* 2005, **32**, 539-551.
39 M. R. Lutfor, A. Jahimin, S. Kumar, S. Silong and M. Z. Rahman, *Phase Trans*., 2009, **82**, 228-239.
40 M. R. Lutfor, H. C. Kwong, M. Y. Mashitah, G. Hegde, M. M.T, Ibrahim and M. A. R. Zaki, *Acta. Cryst*., 2012, **68**, 02958.
41 M. R. Lutfor, G. Hegde, S. Kumar, C. Tschierkeand V. G. Chigrinov, *Opt. Mater*., 2009, **32**, 176-183.
42 S. K. Prasad, K. L. Sandhya, G. G. Nair and D. S. Shankar Rao, *Curr. Sci.,*2004, **86**, 815-823.
43 S. K. Prasad, K. L. Sandhya, D. S. Shankar Rao and Y. S. Negi, *Phys. Rev.,*E2003, **67**, 051701.
44 O. Tsutsumi, T. Kitsunai, A. Kanazawa, T. Shiono, and T. Ikeda, *Macromol.*, 1998, **31**, 355-359.
45 (a) K. Praefckeand D. Blunk, *Liq.Cryst*., 1993, **14**, 1181-1187; (b) K. Praefcke, P. Marquardt, B. Kohne and W. Stephan, *J. Carbo. Chem*., 1991, **10**, 539-548.
46 J. W.Goodby, V. Görtz, S. J. Cowling, G. Mackenzie, P. Martin, D. Plusquellec, T. Benvegnu, P. Boullanger, D. Lafont, Y. Queneau, S. Chambert and J. J. Fitremann, *Chem. Soc. Rev*., 2007, **36**, 1971-2032.

Graphical abstract

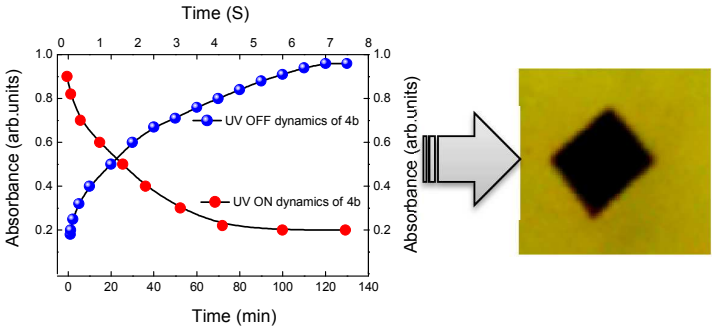

A new myo-inositol based liquid crystal can be used for creation of optical storage devices. Dark area is the UV irradiated area to form disordered isotropic phase whereas bright area is protected from the light by using mask remains in least ordered phase.